A simple finite element model for reactive sputter-deposition systems

by F. Jones
J. S. Logan

The method of finite element analysis is used to calculate oxygen-concentration profiles and oxygen-absorption rates at the substrate and along the shields in an rf magnetron reactive sputtering system having a 12-inch-diameter magnetron. Results for several shield arrangements are calculated as a function of oxygen flow rate. The approach used assumes the following: (i) The target is being sputtered in the metallic state; (ii) the oxygen-concentration profile in the system can be calculated from the diffusion equation; (iii) the maximum amount of oxygen that can be absorbed at any point in the system is proportional to the metal deposition rate at that point; (iv) the target absorbs no oxygen as long as it is in the metallic state. The relative metal deposition rate along the substrate and shields is calculated, normalized to the measured deposition rate at the substrate, and used as a boundary condition for the diffusion equation. The calculated oxygen flow rate for the formation of stoichiometric substrate films agrees with experimental results to within 15%. The critical flow rate at which the target oxidizes, Q_c, is measured experimentally and when used in the model gives an oxygen partial pressure of about $0.31 \cdot 10^{-6}$ torr at the sputtering track.

©Copyright 1990 by International Business Machines Corporation. Copying in printed form for private use is permitted without payment of royalty provided that (1) each reproduction is done without alteration and (2) the *Journal* reference and IBM copyright notice are included on the first page. The title and abstract, but no other portions, of this paper may be copied or distributed royalty free without further permission by computer-based and other information-service systems. Permission to *republish* any other portion of this paper must be obtained from the Editor.

Introduction

Reactive sputter deposition is a thin-film deposition technique often used to fabricate thin oxide and nitride films. The method is used when the desired compound target cannot be easily fabricated, when the target is not stable under the desired sputtering conditions, or when the fabrication of the compound target is simply too costly. Targets used in reactive sputter deposition are usually metals, metal alloys, or semiconductors. Most metal and metal alloy targets are readily fabricated because they are highly malleable and can be easily rolled and machined to the desired shapes. In our study, the desired film was ZrO_2. Hence, a zirconium target was used.

In the reactive sputter deposition of ZrO_2, the Zr target is typically sputtered in an argon–oxygen mixture. The compounds formed may or may not be stoichiometric. Stoichiometric films are formed at the substrate when the ratio of the reactive gas arrival rate to the arrival rate of the metal exceeds a value determined from the flux of gas

atoms striking the surface and the sticking coefficient of the reactive gas.

The reactive gas also reacts with the target, tending to form suboxides on its surface. This compound layer is also sputter-etched during the sputtering process. If the compound sputter-etch rate is higher than the compound-formation rate, the target's surface remains in the metallic state. If the compound-formation rate exceeds its sputter-etch rate, the surface of the target is always covered with a compound during the sputtering process. The oxygen flow rate Q at which this occurs is denoted Q_c. The above cases can be achieved by decreasing or increasing, respectively, the flow rate of the reactive gas into the system. Reactive sputter deposition with the target in its compound state is the usual mode of operation when it is necessary to deposit stoichiometric films on the substrate, since enough reactive gas can be introduced into the system to make the surface layer of the target nearly stoichiometric during the sputtering process. This surface layer can never be completely stoichiometric, since the sputter yields of Zr and O atoms are different. However, one might expect that the composition of the surface layer on the Zr target would be similar to what one would find for the surface layer of a ZrO_2 target that is sputter-etched at the same rate.

The sputtering rates of compounds are generally slower than those of the corresponding metals. Consequently, the formation of an oxide on the surface layer of the target is accompanied by a drop in the growth rate of the film deposited on the substrate.

Oxide films also have higher secondary-electron-emission coefficients than do metal films. Hence, the formation of oxides on the target surface when Q exceeds Q_c is accompanied by more secondary electrons being ejected from the target per incident ion. The increased number of secondaries produces more ionization events in the plasma, leading to a denser plasma. At constant target power, an increase in plasma density causes a decrease in target voltage. An increase in the number of secondary electrons, at constant power, also results in a voltage drop. The increase of both plasma density and secondary-electron emission results in a change in target voltage that is easily observable and that can be used as an indication that a radical change in the chemical composition of the target's surface has occurred. This radical change in chemical state of the target with the associated change in target voltage is called the reactive sputter-deposition transition. The oxygen flow rate at the transition point, Q_c, is called the critical oxygen flow rate of the reactive sputter transition.

Several investigators [1–4] have modeled the reactive sputter-deposition transition. Most of the models deal primarily with processes occurring at the target. Ion bombardment and the relative sputter yields of oxides and metals as functions of target voltage are taken into account. A number of other investigators [5] include an averaged surface area, in an attempt to represent the gettering action by metal deposited on the walls of the vacuum chamber. However, these treatments do not give detailed information on the local variation of reactive gas concentration throughout the system or local reactive gas-absorption rates by metal sputtered onto surfaces in the system.

The long-range objective of our work is to develop a model that can be used to calculate reactive gas concentrations and fluxes at all points in reactive sputter-deposition systems designed for experimental and practical use. Although the present model is limited in the range of physical phenomena that it can describe, this paper represents the first time that the method of finite elements has been used to model the reactive sputter-deposition process. Models are now being developed to include other important aspects of the process.

The present model is primarily concerned with processes at the substrate and shields. In this regard, it is different from other models of the reactive sputter-deposition process. The solution is obtained by solving the oxygen-diffusion equation in the sputtering system. Mixed boundary conditions exist on some of the surfaces in the system, making an analytic solution difficult. Hence, a finite element (or finite difference) approach is necessary. Descriptions of the approach used to solve the diffusion equations by finite element analysis can be found in [6]. Before proceeding with a description of the model and its results, we first describe the experiment and some of the relevant data.

Experimental section

The reactive sputter-deposition system used to deposit ZrO_2 that is modeled in this paper has been described in a previous publication [7], in which the reactive sputter-deposition transition is also discussed. Therefore, many of the details concerning the characteristic behavior of the system and properties of the ZrO_2 films made therein are not repeated here. However, experimental details necessary for an understanding of the model are given below.

ZrO_2 was deposited onto substrates using a reactive sputter-deposition technique developed at the IBM Thomas J. Watson Research Center. A similar technique has been used by Scherer and Wirz [8] to prepare aluminum oxide. A schematic of the system used is shown in **Figure 1** (not drawn to scale). It consists of a vacuum chamber containing a 12-inch-diameter magnetron sputtering source. A Zr target is bonded to the surface of this sputtering source, and the substrate sits below the source. It is surrounded by an enclosure whose function is to concentrate oxygen in the vicinity of the

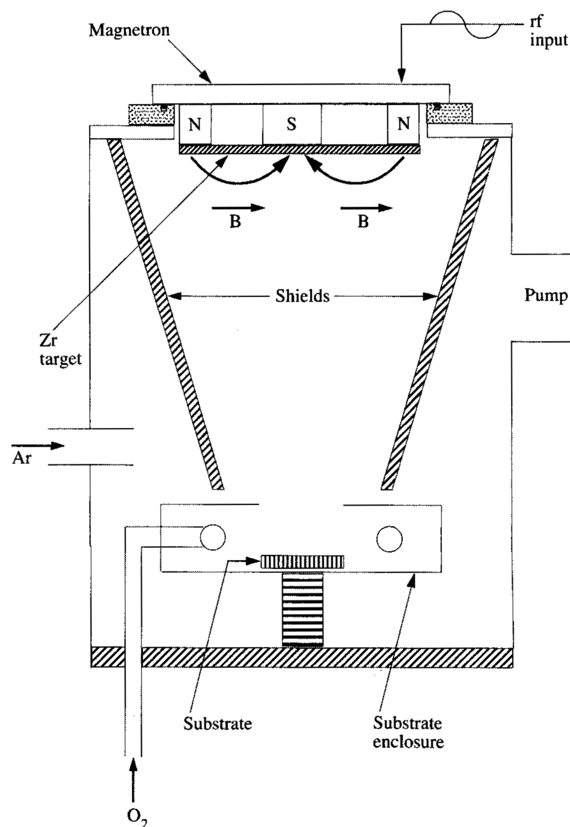

Figure 1

Schematic of rf magnetron reactive sputter deposition system.

substrate. The height of the substrate within the enclosure can be adjusted by placing the sample on 125-mm-diameter disks of varying thickness. In the work described here, the substrate is positioned 6 mm below the aperture of the substrate enclosure. In this location, the film thickness varies by less than ±4% across a 125-mm-diameter substrate. Target–substrate separation can be varied from 197 to 254 mm. The data presented below were collected with a target–substrate separation of 197 mm. Argon is introduced through a stainless steel tube at the side of the chamber. Oxygen is introduced into the system through a gas feed ring that is located inside the enclosure and that surrounds the substrate. The conical shield suspended from the top plate provides an additional surface at which oxygen in the vicinity of the magnetron sputtering source is gettered during the deposition process. Oxidation of the Zr target is undesirable, since the deposition rate of an oxidized target is at least a factor of 10 smaller than that of an unoxidized target.

In earlier work [7], the addition of the conical shield led to a doubling of the amount of oxygen one could let into the system without oxidizing the target. However, more recent experiments by the first author show that the addition of the shield allows one to increase the oxygen flow rate by about one standard cubic centimeter per minute (sccm). This effect is of the order of 5% under the conditions modeled in this paper, where the oxygen flow rate at the transition is about 21 sccm. The reason for the discrepancy is not known at this time.

The sputtering source is driven by an rf power supply. Provisions are made to measure the dc bias voltage of the target and substrate, and the oxygen and argon flow rates are controlled by mass flow controllers to within 0.1 sccm. Except where indicated, the partial pressure of argon during the sputtering process is set to 32 millitorr at the beginning of the deposition process and usually rises to a final pressure of 34 millitorr by the end of the process. The argon flow rate is fixed at 40 sccm. The pumping package consists of a diffusion pump backed by a mechanical roughing pump.

Although the plumbing is not shown, all surfaces of the substrate enclosure are water-cooled and maintained at a temperature of 23°C during the deposition of the film. The magnetron is also water-cooled. The conical shield is not water-cooled and becomes hot during long periods of sputtering.

Rutherford backscattering is used to measure the composition of the films as a function of oxygen flow rate. The thickness of the deposited film is 3000 Å.

Description of the model

In this model, a single diffusion equation is used to calculate the oxygen concentration throughout the system and oxygen absorption rates along the substrate and shields of the system. The film stoichiometry is determined from the ratio of the metal arrival rate and the oxygen absorption rate. Steady-state conditions are assumed to hold. The concentration of oxygen molecules (as shown below) is assumed to be very small in comparison to that of argon. The diffusion constant of molecular oxygen in argon is calculated using the kinetic theory of gases.

The time-dependent diffusion equation is given by

$$\frac{\partial C}{\partial t} = D\nabla^2 C + Q_{\mathrm{Ring}}, \tag{1}$$

where C and D are the oxygen concentration and Ar–O_2 diffusion constant, respectively; Q_{Ring} is a source term representing the flow of oxygen from the gas feed ring. When steady state has been reached, Equation (1) can be written as

$$\nabla^2 C = -\frac{Q_{\mathrm{Ring}}}{D}. \tag{2}$$

From kinetic theory, the Ar–O_2 diffusion constant is given by

$$D = \frac{2}{3\sqrt{\pi}} \frac{1}{P\sigma_0} \sqrt{\frac{(kT)^3}{M_{O_2}}}, \tag{3}$$

where σ_0, P, M_{O_2}, k, and T are the Ar–O_2 collision cross section, argon pressure, mass of the oxygen molecule, Boltzmann's constant, and absolute temperature, respectively. The diameters, d_1 and d_2, of the argon atoms and the oxygen molecules are 2.92 and 2.94 Å, respectively [9]. Using the relation $\sigma_0 = \pi[(d_1 + d_2)/2]^2$, we find σ_0 to be $27 \cdot 10^{-16}$ cm^2. At $T = 300$ K, the calculated values of the diffusion constant at pressures of 32 and 15 millitorr (two typical values) are 3816 and 8141 cm^2/s, respectively. The results of the model are compared for the pressures given above.

Before a unique solution can be obtained for Equation (2), boundary conditions must be specified on the substrate, shields, and target. These boundary conditions are described next.

- *Boundary conditions at the target*

The sputtering source is a magnetron. The magnets are arranged to produce an intense plasma ring very close to the surface of the target. The target sputtering rate in this region is much higher than in other regions, where the plasma has a much lower density. The diameter of the plasma ring is approximately 230 mm, and its width is approximately 6.5 mm. The density of the plasma across the rest of the target is less than that at the ring by at least a factor of 10. Hence, the sputter-etch rate at the ring is at least a factor of 10 greater than in other parts of the target. Eventually, a circular track is etched into the region of the target that is adjacent to the plasma ring.

Because of its low sputter-etch rate, the center portion of the target oxidizes before the sputtering track, as the oxygen flow rate is increased. The sputtering track oxidizes at much higher flow rates. Just below the transition, the sputtering track is in the metallic state, while the center of the target is in the oxide state. The sticking coefficient of O_2 to most oxides is near zero for all practical purposes. Therefore, we assume that oxidized portions of the target do not contribute significantly to the loss of oxygen from the system.

On the other hand, oxygen can react with the metal in the sputtering track. When the target is being sputtered in the metallic mode, the sputter-etch rate of the oxide is so high that any oxygen or suboxides on the target surface are removed immediately. Under these conditions, the absorption rate of oxygen by metal in the sputtering track is insignificant. Therefore, on the target, the boundary condition is given as $dC/dz = 0$, where z is normal to the target's surface. If the oxygen impinging on the sputtering track is resputtered as ZrO_x, where $0 < x < 2.0$, dC/dz is not zero and should be replaced with the proper value. For the finite element solutions discussed in this paper, dC/dz was always set to zero at the sputtering target.

The model described in this paper is not capable of predicting the reactive sputter transition and other effects associated with the transition. Therefore, the solution is valid only for oxygen flow rates less than Q_c. Hence, in these calculations, we assume that the target is always being sputtered in the metallic state.

Another reactive sputter model, developed by one of the authors,* includes the target-sputtering as well as target-oxidation processes. The equations describing the model are solved by the method of finite differences. The finite difference model simulates the target-sputtering process and the metal-gettering processes as oxygen is added to the system. When the oxygen flow rate is high enough, the reactive sputter-deposition transition occurs. Other aspects of the finite difference model are discussed below in the section entitled *Future work.*

- *Boundary conditions on the substrate, shield, and other surfaces*

Let F_{Zr} be the sputtered flux of Zr atoms at a given point at the receiving surfaces (substrate, substrate enclosure, and shield). If the concentration of O_2 molecules adjacent to the surface at this point is C, then the incident flux of O_2 molecules is

$$F_{O_2} = CV_{th}/4, \tag{4}$$

where V_{th} is the mean thermal speed of the oxygen molecules. This is given by

$$V_{th} = (8kT/\pi M_{O_2})^{1/2}. \tag{5}$$

Let S be the oxygen sticking coefficient. The sticking coefficient is the fraction of incident molecules that are absorbed by the Zr atoms arriving at any point along the receiving surfaces. In this model, the sticking coefficient is set to a constant value, S_0, at all points in the sputtering system where the metal arrival rate is greater than the molecular oxygen-absorption rate. The ability of the surface to absorb oxygen molecules is further characterized by a film coefficient, h. The film coefficient, of course, depends on the sticking coefficient. If the oxygen concentration above the surface is C, then the flux of absorbed molecules is

$$F^{Abs} = hC. \tag{6}$$

The relation between F^{Abs} and F_{O_2} is

$$F^{Abs} = SF_{O_2}, \tag{7}$$

or

* F. Jones, IBM Thomas J. Watson Research Center, work in progress.

$$hC = SCV_{th}/4. \quad (8)$$

Hence,

$$h = SV_{th}/4. \quad (9)$$

Let F_{Zr} be the sputtered flux of Zr atoms at a given point at the receiving surface. Let F^{Abs}_{max} be the maximum flux of oxygen molecules that can be absorbed by the film at a given point during the deposition process. Let the corresponding concentration be C_M. The formula for completely reacted zirconia is ZrO_2. It follows that F^{Abs}_{max} at a given point is equal to F_{Zr} at that point. We use the following relationship between F^{Abs}_{max}, the film coefficient h, and C_M:

$$F^{Abs}_{max} = hC_M . \quad (10)$$

When the concentration exceeds C_M, the excess flux of oxygen molecules is rejected by the film. Thus, we represent the sticking coefficient as

$$S = \begin{cases} S_0 & \text{for } C \le C_M , \\ \dfrac{S_0 C_{max}}{C} & \text{for } C > C_M . \end{cases} \quad (11)$$

Consequently, when $C > C_M$, h varies with concentration as follows:

$$h = \frac{S_0 C_M V_{th}}{4C} . \quad (12)$$

Since $F^{Abs}_{max} = F_{Zr}$, it follows that

$$C_M = \frac{4F_{Zr}}{S_0 V_{th}} . \quad (13)$$

• *Distribution of metal sputtered onto substrates and shields*

The boundary conditions on the substrate and shield are determined from the metal sputtered onto these surfaces. We use a method of Maissel and Glang [10] to calculate the distribution of sputtered metal. The effects of gas-phase scattering are omitted. The sputtered distribution is calculated for a ring source having inner and outer diameters of 222 mm and 235 mm, respectively. Hence, the width of the sputter ring is 6.5 mm. The separation between target and substrate is 200 mm. The size of the aperture of the substrate holder is variable. Apertures of 102, 114, and 127 mm are used. An inverted conical shield is used in the experiments. The diameters of the openings at the top and bottom of the conical shield are 356 and 188 mm, respectively. The height of the shield is 140 mm. The vertical distance between the bottom edge of the shield and the top surface of the substrate enclosure is 50 mm. As mentioned earlier, the substrate rests on a thick aluminum disk during the deposition. The height of the pedestal is such that the substrate is located 6 mm below the top surface of the substrate enclosure.

The relative thickness distribution of metal sputtered onto (i) the inner surface of the conical shield, (ii) the top surface of the substrate enclosure, and (iii) the substrate was calculated using the model of Maissel and Glang. The relative thickness distribution has a value of 1.0 at the center of the substrate. At an oxygen flow rate of 21 sccm and an rf target power of 3 kW, stoichiometric zirconium dioxide is deposited at the center of the substrate at a rate of 1000 Å/min. The corresponding flux of Zr metal atoms, F_{Zr}, is $4.22 \cdot 10^{15}$ atoms/cm^2. The relative thickness distribution is multiplied by this value of F_{Zr} to obtain the Zr flux at other points within the sputtering system. The openings at the bottom of the conical shield and the top of the substrate enclosure represent apertures in the system. The aperture geometry is included in the calculation of the sputtered metal flux distribution along the inner surface of the conical shield, the top surface of the substrate enclosure, and the surface of the substrate.

• *Effects of the plasma on oxygen transport and sticking coefficient*

Although the plasma is used to sputter zirconium and oxygen atoms from the surface of the target, we neglect its effect on the transport behavior of neutral atoms and molecules as they pass through the system. This is because the plasma density is quite low compared to that of argon. At an argon pressure of 32 millitorr, the argon atom density is about 10^{15} atoms/cm^3. The plasma density near the track is of the order of 10^{11}–10^{12} ions/cm^3. However, high-energy electrons in the plasma can excite, ionize, and break up the oxygen molecules. Such excited species exhibit an enhanced reactivity over that of the unexcited O_2 molecule. In such cases, the sticking coefficient, S_0, is expected to be higher for the excited species than for the unexcited species. The maximum value of the sticking coefficient is 1.0. If the unexcited species already has a sticking coefficient of 1.0, plasma excitation of the species will not increase its sticking coefficient. However, if the unexcited species has a sticking coefficient that is less than 1.0, the sticking coefficient will increase. Except where indicated, the value of the sticking coefficient is set to 1.0.

Model layout

In our finite element analysis, the system to be modeled is divided into a grid consisting of rectangular and triangular cells called *elements*. The vertices of the cells are called *nodes*. Internal sources of oxygen are specified at some nodes of the elements. The specification of fluxes and concentrations at boundaries leads to a unique solution to the differential equation. The differential

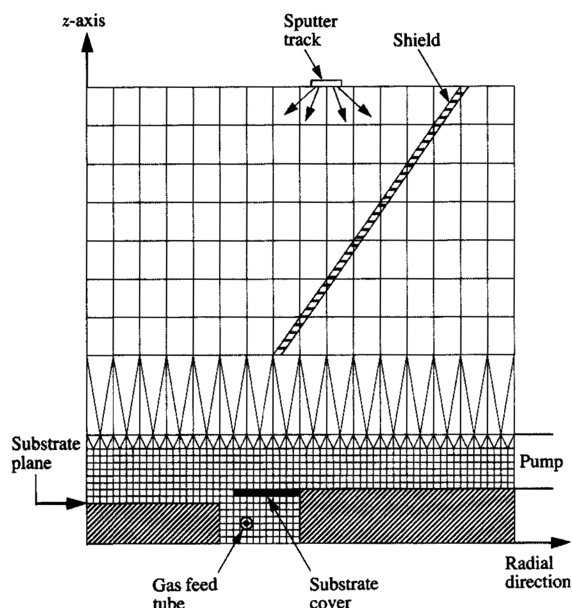

Figure 2

Finite element geometry representing the reactive sputter-deposition system.

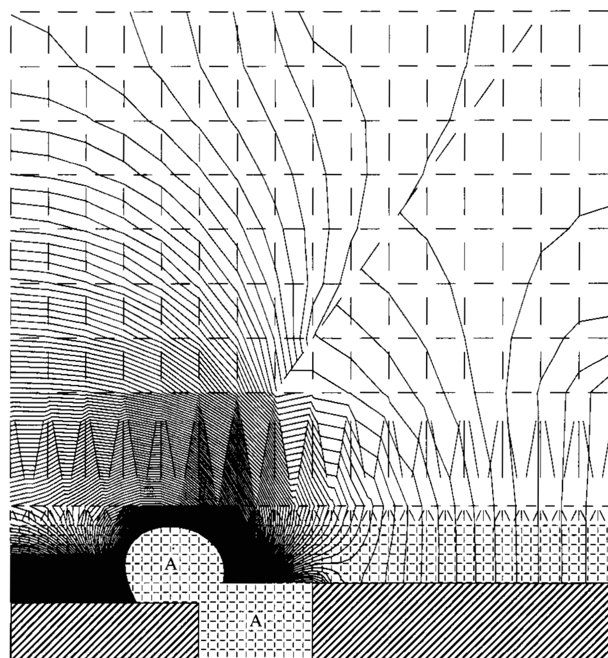

Figure 3

Oxygen concentration contours for 100 evenly spaced values of oxygen concentration. Minimum values occur along the inner surface of the conical shields and near the vacuum pump. Concentration values increase as the substrate is approached. Contours not plotted in region A, where concentration is greater than $2.9 \cdot 10^{12}$ molecules/cm^3.

equation is solved at the nodes. The solution between nodes is found by interpolation. Fluxes across the boundaries of an element are calculated from the product of the diffusion constant and the concentration gradient at the boundary.

A cross section of the cylindrically symmetric finite element grid chosen to simulate the system is shown in **Figure 2**. The layout is slightly different from that of Figure 1 in the following respects. In the model, a 406-mm-diameter vacuum chamber is used instead of the 508-mm chamber used in the experiment. This significantly reduces the amount of computation without producing significant changes in the solution.

The system vacuum pump is represented by the "pump" drawn at the seven nodes shown in the figure. The pump used in the model has cylindrical symmetry with respect to the *z*-axis, although the pump used in the actual system is located on one side of the chamber. When the target is being sputtered in its metallic state, most of the oxygen is removed from the system by chemical reactions with the metal sputtered onto the surfaces of the system. Experimentally, it is observed that when the target is sputtered in the metallic mode, the pressure of the system does not change significantly with increasing oxygen flow rates. This is true even for oxygen flow rates as high as that of argon. This experimental result suggests that the pump does not play a major role in removing oxygen from the system. The finite element solution shows that the axisymmetric pump removes about 5% of the oxygen supplied to the system. These results suggest that when diffusion is the primary mode of transport, the geometry of pumps located at the edge of large oxide-reactive sputtering systems may not significantly affect the final result. However, one would expect the pump location and geometry to become more and more important as the size of the system decreases.

The locations of the shield, substrate, substrate enclosure, target sputtering track and gas feed ring are as shown in Figure 2. The solutions show the effects of the conical shield position, substrate aperture size, and argon pressure. These results are presented next.

Solutions of the finite element model

• *Concentration and oxygen absorption rates as calculated by the finite element model*

In the following, different levels of complexity and detail of the solution obtained by finite element analysis are

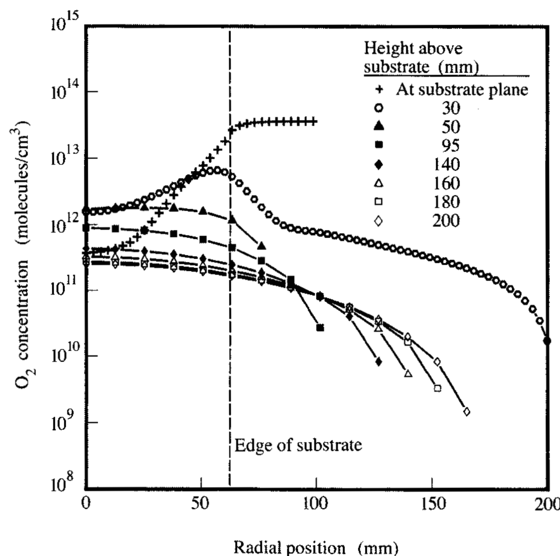

Figure 4

Oxygen-concentration profiles at the plane of the substrate (pluses) and at different heights above the substrate.

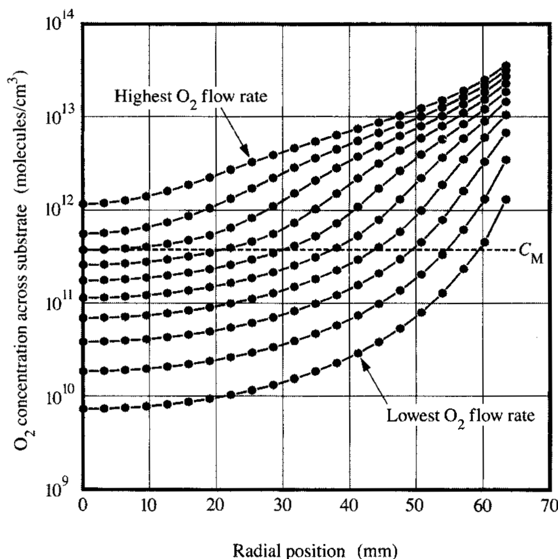

Figure 5

Oxygen-concentration profiles across the substrate at ten oxygen flow rates. From the lowest curve to the top curve, the flow rates are 2.5, 5.0, 7.5, 10.0, 12.5, 15.0, 17.5, 20.0, 22.5, and 25.0 sccm of oxygen, respectively.

illustrated. **Figure 3** shows concentration contours for 100 values of oxygen concentration in the system, plotted for an oxygen flow rate of 20 sccm. The minimum values of concentration occur along the inner surface of the shield, top surface of the substrate enclosure, and near the vacuum pump. The concentration increases as one approaches the substrate. The minimum and maximum values plotted are $8.5 \cdot 10^9$ and $2.9 \cdot 10^{12}$ molecules/cm^3, respectively. (There is nothing special about these values. They were chosen to help delineate some of the features of the finite element solution).

Plots such as that shown in Figure 3 are useful in viewing gross features of the solution and obtaining insight into the general behavior of the system. Figure 3 shows that when the gas passes through the narrow channel between the edge of the substrate holder and the aperture plate of the substrate enclosure, semi-toroidal concentration contours are created. In order to illustrate these contours more clearly, we selected a typical value of $2.9 \cdot 10^{12}$ molecules/cm^3 and displayed in Figure 3 only those contours with lower concentrations. Region A, for which the contours are not plotted, has higher values of concentration. Note that the contours near $2.9 \cdot 10^{12}$ start on the substrate and end on the aperture plate. Another observation is that the oxygen concentration is greater in the center of the target than it is near the edge of the target. This effect is created by the gettering action of the conical shield. Finally, along the outer surface of the conical shield, the contours end perpendicular to the surface (except in the lowest element, where a discontinuity in the boundary condition exists at the lowest point of the shield). This is because no metal is sputtered onto the outer surface of the cone. Hence, all oxygen molecules striking the outer surface of the cone are reflected; this is equivalent to saying that $dC/dz = 0$ on the outer surface of the cone.

Although Figure 3 is useful for viewing gross features of the finite element solution, more quantitative information can be obtained by plotting concentration and flux profiles. **Figure 4** shows radial variations of molecular oxygen concentration in the plane of the substrate and at different heights above the substrate. (The oxygen flow rate is $Q = 20$ sccm.) The concentration along the substrate has its lowest value at the center of the substrate and increases with increasing radius. The edge of the substrate is located a distance of 63 mm from the center. The concentration at the substrate plane levels off with increasing radius and shows that the O_2 concentration is almost constant under the substrate enclosure. Although the concentration adjacent to the substrate shows a radial variation, the oxygen flow rate is high enough to produce a stoichiometric film at every point on the substrate. The curve drawn with open circles passes through the semi-

toroidal region. Hence, the concentration rises as the semi-toroidal region is approached from either side. The open circles show an almost linear fall-off as the pump is approached. However, at a distance of about 20 mm from the pump, the concentration falls rapidly. The other curves show concentration profiles that start at $r = 0$ and end on the inner surface of the conical shield. The curve drawn with open diamonds shows the concentration variation along the surface of the target. In all cases, the initial decrease in concentration with radius is relatively slow but becomes faster as the shield is approached.

Figure 5 shows how the oxygen concentration varies with radial position along the substrate, for ten different oxygen flow rates between 2.5 and 25.0 sccm inclusively. The dashed line indicates the concentration, C_M, at which the deposited film becomes stoichiometric.

From Figure 5, it can be seen that the points near the outer edge become stoichiometric first. With increasing O_2 flow rate, points closer to the center of the substrate become stoichiometric. Eventually, the entire film on the substrate becomes stoichiometric at a flow rate of about 20 sccm. At a given radial position, the concentration above the substrate does not change by much until it exceeds the dashed line, i.e., C_M. After this happens, the concentration increases faster with increasing flow rate. The faster increase in concentration occurs because excess O_2 molecules must be rejected after stoichiometric deposition conditions have been established at a given point along the substrate.

This is demonstrated more clearly in **Figure 6**, where the oxygen concentration at the center of the substrate is plotted as a function of increasing flow rates. The dashed line at $3.78 \cdot 10^{11}$ molecules/cm^3 represents the concentration at which the film becomes stoichiometric. At $T = 300$ K, this corresponds to an O_2 partial pressure above the center of the substrate of $11.74 \cdot 10^{-6}$ torr.

Of particular importance is the oxygen concentration at the center of the sputtering track as a function of O_2 flow rate. **Figure 7** shows how the concentration of oxygen at the sputtering track varies with oxygen flow rate. This information should be useful to investigators who create models that are used to simulate the target oxidation process as a function of oxygen flow rate. The accuracy of such models depends on knowing how the flux of O_2 molecules bombarding the sputtering track varies as the flow rate is increased. We can readily calculate the flux from Figure 7, using kinetic theory. The surface of the target oxidizes at an oxygen flow rate of about 21.5 sccm. The corresponding concentration is $9.9 \cdot 10^9$ molecules/cm^3. This implies an O_2 partial pressure of $0.31 \cdot 10^{-6}$ torr. The corresponding flux is $1.1 \cdot 10^{15}$ molecules/s-cm^2.

Figure 8 is a plot of F^{Abs} versus r along the substrate ($r < 63$ mm), and along the shield ($r > 63$ mm) for ten

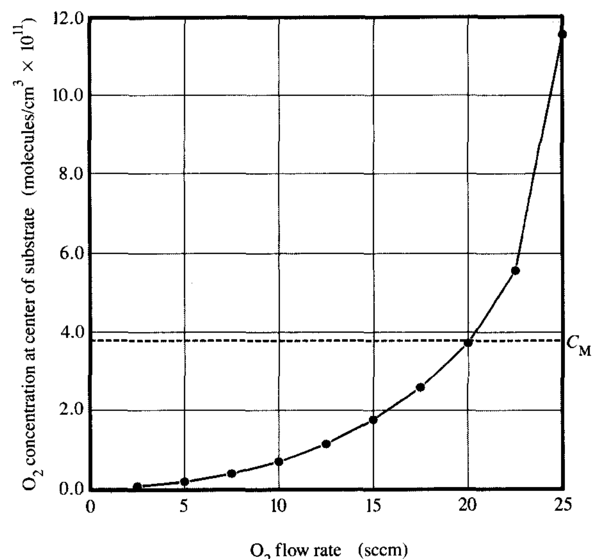

Figure 6

Oxygen concentration at center of substrate vs. oxygen flow rate. The dashed line is the concentration at which stoichiometric conditions exist.

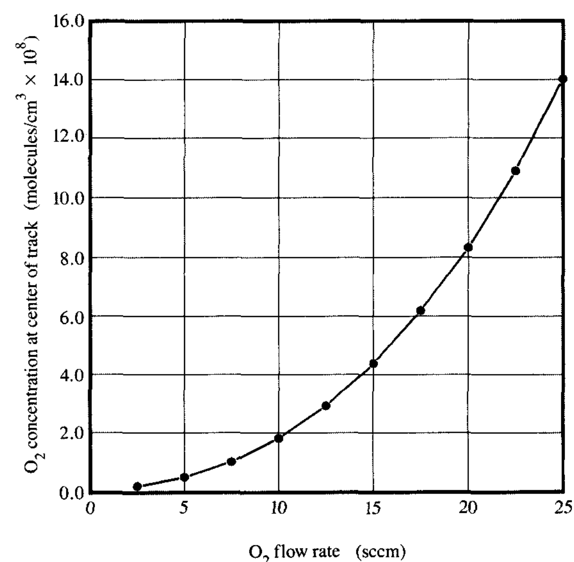

Figure 7

Oxygen concentration in the center of the sputtering track as a function of flow rate.

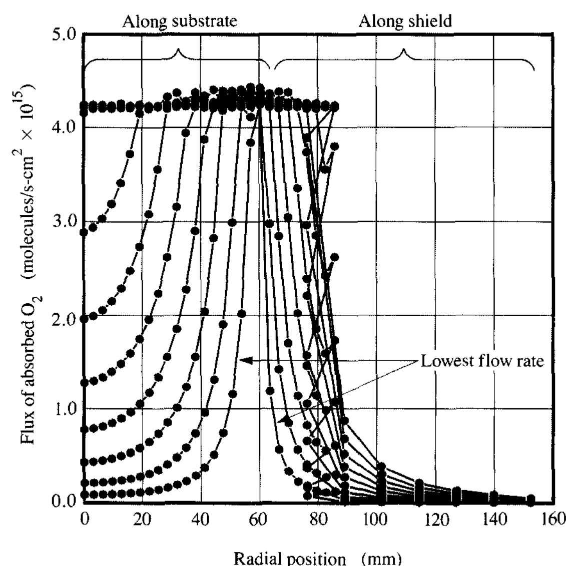

Figure 8

Flux of absorbed oxygen at substrate ($r < 63$ mm) and shield ($r > 63$ mm) for different flow rates. The zigzag at $r = 80$ mm is due to the overlap of conical shield and aperture plate in that region. Ten curves are plotted, but the last two are not visible because of the region overlap. From the lowest curve to the top curve, the flow rates are 2.5, 5.0, 7.5, 10.0, 12.5, 15.0, 17.5, 20.0, 22.5, and 25.0 sccm, respectively.

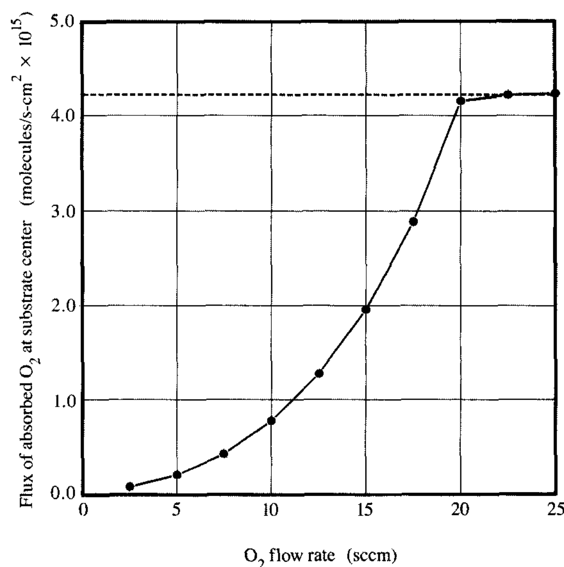

Figure 9

Flux of absorbed oxygen at the center of the substrate. The dashed line represents the absorbed oxygen flux value at which the deposited film becomes stoichiometric.

equally spaced flow rates, starting at 2.5 sccm and ending at 25.0 sccm. The flow rate for the lowest curve is 2.5 sccm. Along the substrate, the height of successive F^{Abs} vs. r curves increases with increasing flow rate until the saturation level is reached. The zigzag of data points around $r = 80$ mm is due to the overlap of the substrate enclosure and conical shield in that region. Although the film deposited on the substrate is stoichiometric above a flow rate of 20 sccm, the film deposited over most of the shield is below stoichiometry, even at a flow rate as high as 25 sccm. Hence, it is not necessary to produce a stoichiometric film at every point in the system in order to produce a stoichiometric film at the substrate.

The center of the substrate is the last place on the substrate to become stoichiometric. Therefore, a plot of the flux of absorbed O_2 molecules at the center vs. oxygen flow rate is of special importance. This is shown in **Figure 9**. The dashed line represents the absorbed flux at which the film in the center of the substrate becomes stoichiometric and consequently has a value of F_{Zr}. The model results plotted in Figure 9 predict that the film should become stoichiometric near an oxygen flow rate of 20 sccm. As is shown below, this prediction is in good agreement with the results obtained from Rutherford backscattering experiments.

- *Effect of geometry and pressure on oxygen concentration*

It is now apparent that the geometry of the system as well as system pressure affects the molecular oxygen-concentration profile throughout the system. System changes that lead to a decrease in the concentration of molecular oxygen at the sputtering track without significantly affecting the concentration at the substrate make it easier to create stoichiometric films at the substrate. This is because a higher oxygen flow rate is required to oxidize the target's sputtering track if such a change is made in the geometry of the system. On the other hand, geometric changes that greatly increase the oxygen concentration along the substrate may also increase the oxygen concentration at the target. Such changes can be quite useful, provided that the increase in concentration near the target does not bring about its oxidation. Higher oxygen flow rates lead to higher oxygen concentration at all points along the substrate, facilitating the formation of a stoichiometric oxide.

The utility of a model, provided it is a close approximation to reality, is that it enables one to predict the effects of different system geometries as well as changes in experimental parameters on film

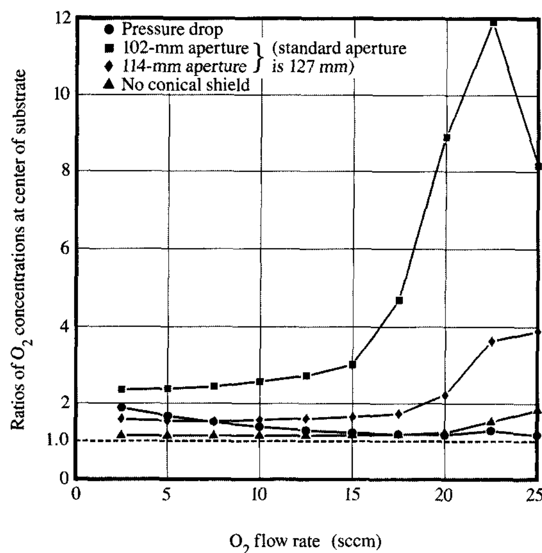

Figure 10

Concentration ratios at center of substrate vs. oxygen flow rates.

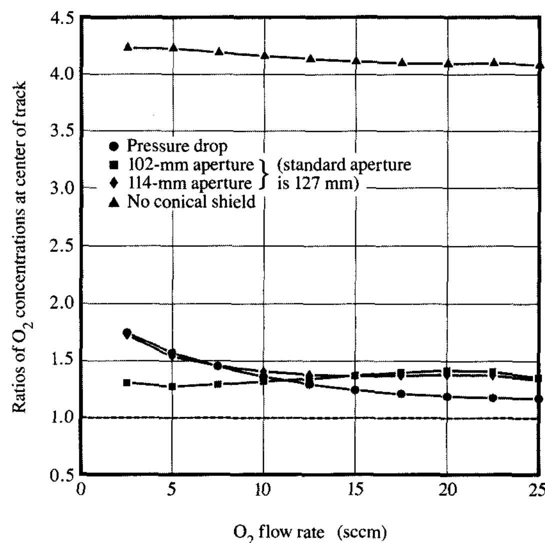

Figure 11

Oxygen-concentration ratios at the center of the sputtering track vs. oxygen flow rate.

stoichiometry and O_2 concentration profiles without actually carrying out the experiment. In comparing two configurations, we calculate the ratios of oxygen concentration and absorbed fluxes of the "new" or "changed" configuration to a "standard" configuration. The ratio is then plotted as a function of oxygen flow rate. In all of the comparisons discussed below, the standard configuration is the conical shield with a 127-mm-diameter opening in the aperture of the substrate enclosure. The argon pressure is 32 millitorr.

In **Figures 10**, **11**, and **12**, the square and diamond curves represent ratios when 102- and 114-mm-diameter apertures are used, respectively. The triangles show the ratios that result when the conical shield is removed. The dots show the ratios when the pressure is dropped from 32 millitorr to 15 millitorr, the corresponding diffusion constants being 3816 and 8140 cm^2/s, respectively.

Figure 10 shows that all of the above changes result in increased O_2 concentration at the center of the substrate. Lowering the pressure results in a higher diffusion constant, which makes it easier for molecules to reach the center of the substrate. Removing the conical shield results in an increased concentration at the center. This is because the conical shield getters the O_2 molecules in the vicinity of the target as well as the substrate. The strongest effects on concentration ratios are produced by reducing the size of the openings in the aperture of the substrate enclosure. The diamond and square curves, which correspond to openings of 114 and 102 mm, respectively, clearly show significant concentration increases relative to the standard case, in which a 127-mm aperture is used. The concentration ratios for the 102- and 114-mm apertures drop and level off, respectively, at the higher flow rates because the concentration at the center of the substrate in the standard case climbs rapidly after stoichiometric deposition conditions are reached, and the rejection of excess O_2 molecules begins.

Figure 11 shows concentration-ratio variations at the center of the sputtering track as the oxygen flow rate is varied. Decreasing the diameter of the substrate aperture results in a slight increase in oxygen concentration at the sputtering track at higher flow rates. At low flow rates, the smaller aperture causes a lower concentration ratio. The crossover occurs around 15 sccm. The variations are related to (i) the flow rate at which significant amounts of excess oxygen are introduced into the system in the 102-mm and 114-mm configurations; and (ii) the broader oxygen distribution produced when the diameter of the aperture is increased. The flow rate dependence of the curves below 15 sccm is due to factor (ii), while the flow rate dependence of the curves above 15 sccm is due to factor (i). A more detailed explanation is somewhat involved and is not discussed in this paper. The drop in pressure from 32 to 15 millitorr results in increased O_2

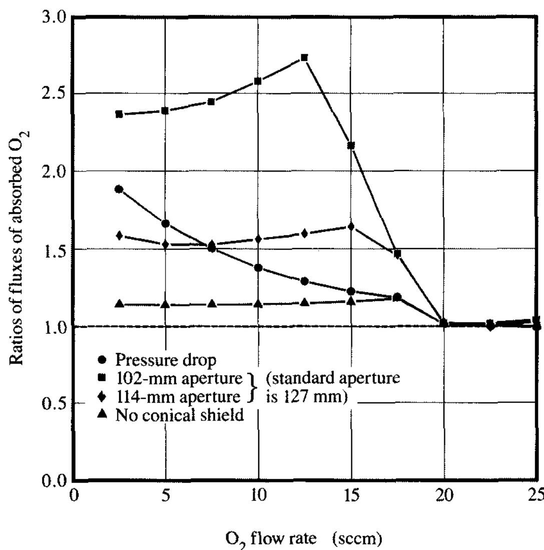

Figure 12

Ratios for absorbed oxygen at substrate center vs. oxygen flow rate.

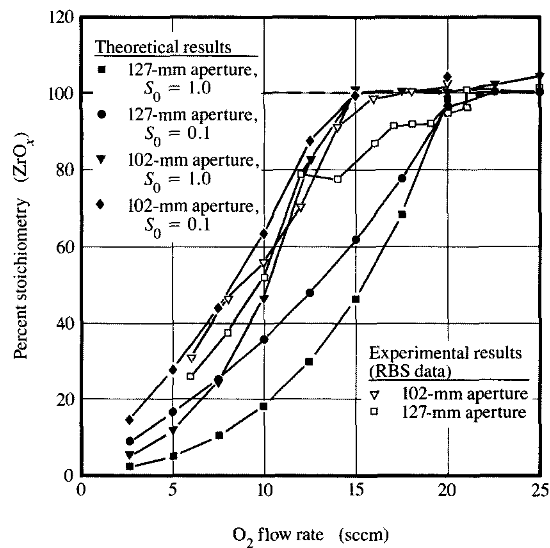

Figure 13

Zirconia percent stoichiometry variations vs. oxygen flow rate.

concentrations at the low flow rates and in lower O_2 concentrations at the higher flow rates. Figure 11 shows that the major effect is caused by the removal of the conical shield. When this is done, the O_2 concentration at the sputtering track increases by more than a factor of 4.3. This increase suggests that the removal of the shield should dramatically affect the oxygen flow rate at which the target oxidizes. However, as mentioned earlier, this is not the case. The most dramatic consequence of removing the shield is the production of opaque and conducting films under almost all conditions for which the full 125-mm-diameter substrate is to be coated (without employing substrate motion). The reason for this discrepancy may lie in the way the boundary conditions are applied in the plane of the target when the shield is removed. Rossnagel [11] has measured significant redeposition of sputtered material onto the target due to gas-phase scattering and back-diffusion. This result means that the target boundary condition should be modified so that it acts as a sink for oxygen. However, the local oxygen-absorption rate in the target plane should depend on the local flux of metal redeposited in the target plane. Berg [5] and others [3, 4] show that in nitride-reactive sputter deposition, the oxidation of the sputtering target depends on the sputter yield of nitride and metal patches on the target. In addition, the target transition point varies roughly as $Y/(X + Y)$, where Y is the nitride or oxide sputter yield and X is the ratio of the nitrogen flux to ion flux at the target. We are currently constructing a new model that includes these as well as other effects. This point is discussed briefly in the section on future work.

Figure 12 shows what happens to the O_2 flux ratios at the center of the substrate when the system configuration and pressure are changed. The strongest effects are caused by decreasing the aperture size of the substrate holder, as shown by the squares and diamonds. Decreasing the pressure also results in higher flux ratios at lower flow rates because of the higher diffusion constant. All of the flux-ratio curves approach 1.0 as the oxygen flow rate increases to 20 sccm, since this is the flow rate at which the film at the center of the substrate is deposited under stoichiometric conditions in the standard configuration.

Comparison of model and experimental results

Rutherford backscattering (RBS) is used to measure the composition of the films deposited at the center of the substrate as a function of O_2 flow rate. The measurements are carried out using 102- and 127-mm-diameter apertures. The argon pressure is held at 32 millitorr. The percent stoichiometry is calculated by dividing the atomic oxygen areal density by twice the Zr areal density and multiplying the result by 100. The results are plotted in **Figure 13**. The open dels and open squares are plots of percent stoichiometry calculated from

the RBS data for the 102- and 127-mm-diameter apertures, respectively. Four curves calculated using the finite element model are also plotted in Figure 13. The percent stoichiometry values in the model calculations are obtained by dividing the flux of absorbed O_2 molecules by F_{Zr} and multiplying the product by 100. For each aperture size, two values of S_0 are used in calculating the film stoichiometry. The solid square and dot curves represent the calculated results for the 127-mm-diameter aperture at S_0 values of 1.0 and 0.1, respectively. Similarly, the solid del and diamond symbols represent the calculated results for a 102-mm-diameter opening at S_0 values of 1.0 and 0.1, respectively.

In the case of the 102-mm aperture, the agreement between theory and experiment is reasonably close, even when the value of S_0 is changed by an order of magnitude. However, a significant difference exists between model results and experimental results for the 127-mm aperture. Decreasing S_0 from 1.0 to 0.1 gives better agreement (see dot curve). It is expected that smaller sticking coefficients will decrease the oxygen-absorption rate at the edge of the substrate and consequently allow more oxygen to diffuse to the center of the substrate. Hence, at low flow rates, more oxygen is absorbed at the center of the substrate when the sticking coefficient is reduced. However, reducing the sticking coefficient below 0.1 causes Q_s, the calculated oxygen flow rate required to oxidize the film deposited at the center of the substrate, to shift to higher values. At the same time, the agreement between theory and experiment worsens.

It appears that, despite the discrepancy in the case of the 127-mm aperture, the model closely predicts the O_2 flow rate needed to produce a stoichiometric film at the center of the substrate. From the RBS data, we can determine that the flow rates needed to produce stoichiometric films for the 102- and 127-mm-diameter apertures are 17 and 21 sccm, respectively. The calculated flow rates are 15 and 20 sccm, respectively. The percent deviations of the calculated flow-rate values from the measured values are 15% and 5%, respectively.

Future work

The simple finite element model described above gives insight into reactive sputter deposition. However, other phenomena must be included in order to more accurately model reactive sputter-deposition processes for oxides. Hence, the authors are currently extending the model to include the following features for small as well as large reactive sputter-deposition systems: (1) combined Monte Carlo and diffusion models of gas-phase transport of sputtered metal atoms, (2) gas-phase chemical reactions and transport of reaction products, (3) oxidation processes at the sputtering target, (4) local plasma-density variations across the surface of the sputtering target, and (5) flow as well as diffusional transport of species within the system. Extensions 1, 2, and 3 have already been completed, and a manuscript describing the results is under preparation.* Possible models for (4) are currently being considered. A Navier–Stokes finite difference solution scheme is being investigated for flow-diffusion effects of reactive as well as nonreactive species.

Summary

The diffusion equation is used to describe oxygen transport in a zirconium-dioxide-reactive sputter-deposition system. The sputtering source is an rf magnetron to which a Zr target has been bonded. Zr metal sputtered onto the substrate and shield reacts with oxygen introduced into the system to form ZrO_2 at the substrate. The substrate rests on an aluminum pedestal inside a cavity through which oxygen must pass before it enters the other parts of the system. The oxygen flow rate can be adjusted to a level at which all the Zr metal deposited on the substrate is fully oxidized. Rutherford backscattering is used to measure film composition vs. oxygen flow rate. The finite element model described in this paper includes all of the above system features. The model closely predicts the oxygen flow rate needed to completely oxidize the Zr metal uniformly deposited onto a 125-mm-diameter silicon substrate. The finite element solution agrees well with the experimental results obtained in the case where the substrate aperture has a diameter of 102 mm. On the other hand, the model predictions for a 127-mm-diameter aperture clearly demonstrate the need for an improved model. Nevertheless, the model predicts, to within 15%, the flow rate needed to make stoichiometric films. In view of the number of approximations in the model, the qualitative agreement between the model and experimental results is good.

Improvements to the current model have already been implemented. These include (1) a combined Monte Carlo/diffusion transport model for the sputtered metal atoms, (2) target oxidation processes, and (3) gas-phase chemical reactions. The reactive sputter-deposition model that includes items 1, 2, and 3 has been solved using the method of finite differences, and a manuscript describing the results is under preparation.

Acknowledgments

The authors would like to thank Grant Coleman for the Rutherford backscattering measurements. They also acknowledge Richard Ghez and Ajay Sharma for useful comments and discussions.

* F. Jones, IBM Thomas J. Watson Research Center, work in progress.

References

1. A. Eltoukhy, B. Natarajan, and J. Green, "Mechanisms of Reactive Sputtering of Indium: III. A General Phenomenological Model for Reactive Sputtering," *Thin Solid Films* **69**, 229 (1980).
2. T. Abe and T. Yamashima, "The Deposition Rate of Metallic Thin Films in the Reactive Sputtering Process," *Thin Solid Films* **30**, 19 (1975).
3. F. Shinoki and A. Itoh, "Mechanisms of Reactive Sputtering," *J. Appl. Phys.* **46**, No. 8, 3381 (1975).
4. J. Affinito and R. Parsons, "Mechanisms of Voltage Controlled, Reactive, Planar Magnetron Sputtering of Al in Ar/N_2 and Ar/O_2 Atmospheres," *J. Vac. Sci. Technol. A* **2**, No. 3, 1275 (1984).
5. S. Berg, H.-O. Blom, M. Moradi, C. Nender, and T. Larrson, "Process Modeling of Reactive Sputtering," *J. Vac. Sci. Technol. A* **7**, No. 3, 1225 (1989).
6. David S. Burdett, *Applied Finite Element Analysis*, Addison-Wesley Publishing Co., Reading, MA, 1988.
7. Fletcher Jones, "High-Rate Reactive Sputter Deposition of Zirconium Dioxide," *J. Vac. Sci. Technol. A* **6**, No. 6, 3088 (1988).
8. M. Scherer and P. Wirz, "Reactive High Rate D.C. Sputtering of Oxides," *Thin Solid Films* **119**, 203 (1984).
9. L. Maissel and R. Glang, *Handbook of Thin Film Technology*, McGraw-Hill Book Co., Inc., New York, 1983.
10. *CRC Hand Book of Chemistry and Physics*, Chemical Rubber Co., Cleveland, OH, 1986.
11. S. Rossnagel, "Gas Density Reduction Effects in Magnetrons," *J. Vac. Sci. Technol. A* **6**, No. 1, 19 (1988).

Received January 19, 1990; accepted for publication May 4, 1990

Fletcher Jones *IBM Research Division, Thomas J. Watson Research Center, P.O. Box 218, Yorktown Heights, New York 10598.* Dr. Jones received a Ph.D. in applied physics from Harvard University in 1975 for his doctoral research on the growth of smectic liquid crystals from isotropic solutions and the smectic-to-nematic phase transition. At Harvard University, he majored in solid-state physics, with a minor in quantum mechanics and a minor in applied mathematics. In 1975, he joined IBM as a Research Staff Member in the electron beam and optical lithography group, developing models for three-dimensional exposure and development of electron beam and optically sensitive resist materials. In 1984, Dr. Jones began his experimental and theoretical studies of the high rate reactive sputter-deposition process. He is a member of the American Physical Society, the American Vacuum Society, and the National Organization of Black Chemists and Chemical Engineers.

Joseph S. Logan *IBM Research Division, Thomas J. Watson Research Center, P.O. Box 218, Yorktown Heights, New York 10598.* Dr. Logan received his B.S. in 1955 and his M.S. in 1956, both from Cornell University, and his Ph.D. in 1961 from Stanford University. He joined IBM in 1960 in Poughkeepsie, New York, where he worked on tunnel diode development and semiconductor surface physics. In 1965, he moved to the General Technology Division at East Fishkill, where he worked on the development of rf sputtered insulators, including the development of a process for the first bipolar memories, substrate tuning of rf sputtering systems, high-frequency (40-MHz) sputtering, and basic understanding of rf sputtering. Between 1973 and 1983, Dr. Logan managed the development base technology group responsible for semiconductor multilevel interconnection technology. This work included polyimide insulator systems, interlevel via technology, interlevel shorts problems, and planar insulator technology. In 1984, he joined the Thomas J. Watson Research Center, where he is manager of Vacuum Process Quality, a part of the Manufacturing Research organization. Dr. Logan is a member of the American Vacuum Society, the Electrochemical Society, the Institute of Electrical and Electronics Engineers, Sigma Xi, and Tau Beta Pi.